

Dicke Phase Transition in a Disordered Emitter-Graphene Plasmon System

Yu-Xiang Zhang,^{*} Yuan Zhang,[†] and Klaus Mølmer[‡]

Department of Physics and Astronomy, Aarhus University, DK-8000 Aarhus C, Denmark

We study the Dicke phase transition in a disordered system of emitters coupled to the plasmonic modes of a graphene monolayer. This system has unique properties associated with the tunable, dissipative and broadband characters of the graphene surface plasmons, as well as the disorder due to the random spatial distribution and the inhomogeneous line-width broadening of the emitters. We apply the Keldysh functional-integral approach, and identify a normal phase, a superradiant phase and a spin-glass phase of the system. The conditions for these phases and their experimental signatures are discussed.

The Dicke model [1], which describes the collective coupling between an ensemble of emitters and a radiation field, implies a superradiant (SR) phase [2, 3] characterized by a non-zero electromagnetic field excitation and a collective atomic polarization [4]. The validity of the theory predicting the SR phase, especially the proper treatment of A^2 [5] and P^2 terms [6], has been questioned, but has been recently clarified [7–11], and the SR phase has now been observed experimentally in cold atom systems [12–17] where an effective Dicke model is constructed via cavity-assisted Raman transitions [18]. The Dicke model and its phase transitions have also been extended to scenarios with multi-mode cavities [19–23], cavity losses [23–25] and time-dependent couplings [26] as well as other systems like superconducting circuits [27, 28], Dicke lattice models [29], etc. These proposals display the richness of phenomena associated with the collective and super-radiant light-matter interaction and stimulate studies of the relation between critical behavior and quantum entanglement [30], quantum chaos [31] and non-equilibrium dynamics [22] in a variety of different physical systems.

In this Letter, we investigate the possibility of observing the Dicke SR phase transition within a system of emitters coupled to surface plasmons (SP). The SP are evanescent electromagnetic modes confined near conductor-dielectric interfaces [32]. Their compressed mode volumes enable strong near-field light-emitter couplings [33, 34], which make quantum plasmonics a promising platform for quantum optical effects [35, 36]. Recent developments of two-dimensional plasmonic materials [37] and, particularly, graphene [38], which can be tuned by means of a gate potential [38–40], motivate us to study the Dicke phase transition in systems with graphene SP, cf. Fig. 1.

The extension of the Dicke model to quantum plasmonics must take into account the broadband SP spectral density [41–43] and the intrinsic Ohmic losses in the graphene. Thus, the quantization of SP is more technical than that of optical cavity modes [44–48]. Moreover, the fact that the graphene SP wavelengths are shorter than

those of free photons by two orders of magnitudes [39], and could be much shorter than the spatial extent of the emitter ensemble, makes it impossible to associate a uniform emitter-field coupling strength as commonly used in the Dicke model. Finally, emitters such as the rare-earth ions doped in crystal, have randomly distributed positions and inhomogeneously broadened transition frequencies. The intrinsic dissipation and disorder will seriously affect the collective coupling to the SP modes and hence the conditions for the SR phase transition, and allow the presence of a quantum spin-glass phase [49].

Theory- To describe the disordered emitter-graphene system illustrated in Fig. 1, we shall establish a Keldysh functional-integral approach, which takes the field losses due to the medium into account [44].

A bosonic field $\mathbf{f}(\mathbf{r}, \tilde{\omega})$, with three Cartesian components (f_a), position \mathbf{r} , and frequency $\tilde{\omega}$, can be defined with the commutators $[f_a(\mathbf{r}_1, \tilde{\omega}_1), f_b^\dagger(\mathbf{r}_2, \tilde{\omega}_2)] = \delta_{ab}\delta(\mathbf{r}_1 - \mathbf{r}_2)\delta(\tilde{\omega}_1 - \tilde{\omega}_2)$, $[f_a, f_b] = 0$ and $[f_a^\dagger, f_b^\dagger] = 0$, such that the quantized electric field can be written as [46–48]:

$$\mathbf{E}(\mathbf{r}) = i\mu_0 \sqrt{\frac{\hbar\epsilon_0}{\pi}} \int_0^\infty d\tilde{\omega} \int d^3\mathbf{r}' \times \tilde{\omega}^2 \sqrt{\Im\epsilon(\mathbf{r}', \tilde{\omega})} \mathbf{G}(\mathbf{r}, \mathbf{r}', \tilde{\omega}) \cdot \mathbf{f}(\mathbf{r}', \tilde{\omega}) + h.c., \quad (1)$$

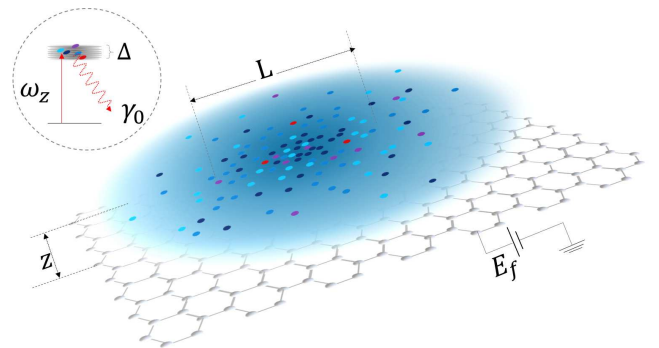


Figure 1. Emitter-graphene system. An ensemble of N emitters with spontaneous emission rate γ_0 and transition frequency inhomogeneously broadened by Δ around a central transition frequency ω_z , is distributed in a layer with horizontal dimension L at height z . The Fermi energy E_f of the graphene electrons can be tuned by gate doping.

^{*} iyxz@phys.au.dk

[†] yzhang@phys.au.dk

[‡] moelmer@phys.au.dk

where $\mathbf{G}(\mathbf{r}, \mathbf{r}', \tilde{\omega})$ is the dyadic Green's tensor, μ_0 and ϵ_0 are the vacuum susceptibility and permittivity, \Im stands for the imaginary part of the relative permittivity, and *h.c.* is short for 'Hermitian conjugate'. Equation (1) resembles the particular solution to Maxwell's equations associated with a quantized current source $\tilde{\omega} \sqrt{\hbar \epsilon_0 \Im \epsilon(\mathbf{r}', \tilde{\omega}) / \pi} \mathbf{f}(\mathbf{r}', \tilde{\omega})$.

The Hamiltonian of the system studied by us can be written as

$$H = H_0 + \sum_{i=1}^N \left[\frac{1}{2} \hbar \omega_{i,z} \sigma_i^z - \sigma_i^x \mathbf{d}_i \cdot \mathbf{E}(\mathbf{r}_i) \right], \quad (2)$$

where $H_0 = \int d^3 \mathbf{r}' \int_0^\infty d\tilde{\omega} \hbar \tilde{\omega} \mathbf{f}^\dagger(\mathbf{r}', \tilde{\omega}) \mathbf{f}(\mathbf{r}', \tilde{\omega})$ is the free field Hamiltonian, $\omega_{i,z}$, \mathbf{d}_i and \mathbf{r}_i are the transition frequency, dipole and position of the i^{th} emitter. We model the emitters as two-level systems with Pauli operators σ_x^i and σ_z^i . Notice that here the rotating-wave approximation is not used.

The Hamiltonian in the form of Eq. (2) has been widely used in the literature, and should be interpreted within the multipolar gauge and the term $\mathbf{E}(\mathbf{r}_i)$ of Eq. (2) should be understood as $\frac{1}{\epsilon(\mathbf{r}_i)\epsilon_0} \mathbf{D}(\mathbf{r}_i)$, where $\mathbf{D}(\mathbf{r}_i)$ is the displacement field [8–11]. Equation (2) further assumes that the distance between any two emitters is larger than the size of the atoms, since, otherwise, a residual instantaneous interatomic potential must be included in the treatment [10, 11]. Notice that the experimental observations of the SR phase transitions are based on effective Dicke models employing Raman processes [12–18]. Our theory can be generalized straightforwardly to the quantum plasmonic version of these models [50].

The Keldysh functional-integral approach is convenient for the analysis of open system non-equilibrium dynamics in disordered systems [22]. To apply it, the Pauli operators representing the two-level emitters are replaced by a real bosonic variable $\phi_i(t)$ restricted to have unit length, i.e., $\phi_i^2(t) = 1$ [22]:

$$\sigma_i^x(t) \rightarrow \phi_i(t), \quad \sigma_i^z(t) \rightarrow \frac{2}{\omega_{i,z}^2} (\partial_t \phi_i)^2 - 1. \quad (3)$$

This mapping originates from the correspondence between the energy gap of quantum models and the correlation length along the 'time' direction of their classical counterparts, and works well for phase transitions [21–24], see Refs. [51–54] for further details. The Keldysh action of the free emitters derived from Eq. (2) is then expressed as

$$S_e = - \sum_{\substack{i=1 \\ a=\pm}}^N \int_{C_a} dt \left[\frac{1}{\omega_{i,z}} (\partial_t \phi_{i,a})^2 + \lambda_{i,a}(t) (\phi_{i,a}^2 - 1) \right], \quad (4)$$

where $\lambda_{i,a}$ is the Lagrange multiplier introduced for the restriction $\phi_{i,a}^2 = 1$, and the variables labelled by $a = \pm$ are defined along the time-integral contours $C_\pm = \mp\infty \rightarrow \pm\infty$ (for steady states, we do not need to specify initial states [55]).

In the Keldysh functional integral approach, we can formally integrate out the degrees of freedom of $\mathbf{f}(\mathbf{r}, \tilde{\omega})$ and get the Keldysh action for the emitter-emitter coupling mediated by them [56]:

$$S_{ee}^{(p)} = \sum_{i,j=1}^N \int_{-\infty}^{\infty} \frac{d\omega}{2\pi} (\phi_{i,c} \quad \phi_{i,q})_{-\omega} \times \begin{pmatrix} 0 & h_{ij}^*(\omega) \\ h_{ij}(\omega) & 2i\Im h_{ij}(|\omega|) \end{pmatrix} \begin{pmatrix} \phi_{j,c} \\ \phi_{j,q} \end{pmatrix}_{\omega}, \quad (5)$$

where the ω -dependent coupling strength is

$$h_{ij}(\omega) = \frac{\omega^2}{2\hbar\epsilon_0 c^2} \mathbf{d}_i \cdot \mathbf{G}(\mathbf{r}_i, \mathbf{r}_j, \omega) \cdot \mathbf{d}_j. \quad (6)$$

Note that we have passed to the Fourier domain with frequency variable ω , and have transformed to the so-called 'classical' ('quantum') fields $\phi_{i,c(q)}$ by the Keldysh rotation $\phi_{i,c(q)} = [\phi_{i,+} + (-)\phi_{i,-}]/\sqrt{2}$ [22]. The corresponding transformation of the Lagrange multipliers $\lambda_{i,c(q)}$ is $\lambda_{i,c(q)} = \lambda_{i,+} + (-)\lambda_{i,-}$.

Spatial Disorder—To treat the disorder in the emitter system, we follow the strategy of random-bond models widely used in the studies of spin-glasses [57]. That is, the real and imaginary parts of the coupling strength, $\{\Re h_{ij}(\omega), \Im h_{ij}(\omega)\}_{i \neq j}$, which are functionals of the emitter positions and dipoles, are viewed as random variables following a multi-component Gaussian distribution (neglecting higher order moments) with the mean and the covariance given by

$$\bar{h}_{(2)}(\omega) = \int d^3 \mathbf{r}_a d^3 \mathbf{r}_b p(\mathbf{r}_a, \mathbf{r}_b) h_{ab}(\omega), \quad (7a)$$

$$M(\omega, \omega') = \int d^3 \mathbf{r}_a d^3 \mathbf{r}_b p(\mathbf{r}_a, \mathbf{r}_b) \times \begin{pmatrix} \delta \Re h_{ab}(\omega) \delta \Re h_{ab}(\omega') & \delta \Re h_{ab}(\omega) \delta \Im h_{ab}(\omega') \\ \delta \Im h_{ab}(\omega) \delta \Re h_{ab}(\omega') & \delta \Im h_{ab}(\omega) \delta \Im h_{ab}(\omega') \end{pmatrix}, \quad (7b)$$

where $p(\mathbf{r}_a, \mathbf{r}_b)$ denotes the probability distribution of the positions of two emitters (the average over $\{\mathbf{d}_i\}$ is implicitly assumed), and 'δ' denotes the difference with respect to the mean value of the real and imaginary parts of $\bar{h}_{(2)}(\omega)$. For the emitter-graphene system to be investigated later, the individual terms $h_{ii}(\omega)$ are identical for all i , since they are determined only by the height z of the emitter layer over the graphene. We shall denote their values as $\bar{h}_{(1)}(\omega)$.

Inhomogeneous Broadening—Emitters such as rare-earth ions doped in crystals experience inhomogeneous broadening of their transition spectrum, cf. Fig. 1. To take this into account, the conventional method is to divide the ensemble into groups of emitters with same transition frequency [29, 58]. Here, we do not follow this method but rather assume the transition frequency $\omega_{i,z}$ follows a Gaussian distribution centered at ω_z with standard deviation Δ . Thus, the broadening can be treated statistically and contributes a new term to the Keldysh

action of the system

$$S^{(b)} = i \frac{\Delta^2}{2\omega_z^4} \sum_{i=1}^N \left(\int d\omega \omega^2 \phi_{i,c}(-\omega) \phi_{i,q}(\omega) \right)^2. \quad (8)$$

In Ref. [56] we show that the main effect of $S^{(b)}$ is to shift the covariance $M(\omega, \omega')$ defined in Eq. (7b) by terms that scale as $(\Delta \frac{\omega \omega'}{\omega_z^2})^2$ and are negligible for a large N .

Order Parameters—To distinguish the different phases of the system, we introduce the following order parameters [22–24, 53, 54, 57]:

$$\begin{aligned} Q_{\alpha\beta}(\omega, \omega') &= -i \frac{1}{N} \sum_{i=1}^N \langle \phi_{i,\alpha}(\omega) \phi_{i,\beta}(\omega') \rangle, \\ \psi_\alpha(\omega) &= -\frac{1}{N} \sum_{i=1}^N \langle \phi_{i,\alpha}(\omega) \rangle, \end{aligned} \quad (9)$$

where $\alpha, \beta \in \{c, q\}$. Q_{cq} , Q_{qc} and Q_{cc} are the retarded, advanced and Keldysh Green's functions of the emitters [22], respectively. ψ_c is the average polarization of the emitters. For the steady state, we substitute the ansatz that $\psi_\alpha(\omega) = 2\pi\delta(\omega)\psi_\alpha$, $\lambda_{i,\alpha}(\omega) = 2\pi\delta(\omega)\lambda_{i,\alpha}$, $Q_{\alpha\beta}(\omega, \omega') = 2\pi\delta(\omega + \omega')Q_{\alpha\beta}(\omega)$ and introduce the Edward-Anderson order parameter q_{EA} [21–23, 49, 52, 57] to pin down the spin-glass phase:

$$Q_{cc}(\omega) = Q_{cc}^{reg}(\omega) - i2\pi q_{EA}\delta(\omega), \quad (10)$$

where ‘reg’ labels the regular part. In the time domain, we have $q_{EA} \propto \lim_{t \rightarrow \infty} \frac{1}{N} \sum_i \langle \sigma_i^x(t) \sigma_i^x(0) \rangle$. Thus a finite q_{EA} implies an infinite correlation time of the individual emitter dipoles.

The steady state of the system and the values of the order parameters are determined by the saddle-point equations of the Keldysh action [56]. This leads to the identification of three different phases: the superradiant (SR) phase with $(q_{EA} \neq 0, \psi_c \neq 0)$, the spin-glass (SG) phase with $(q_{EA} \neq 0, \psi_c = 0)$, and the normal phase with $(q_{EA} = 0, \psi_c = 0)$.

Results—We model the system depicted in Fig. 1, as a layer of N emitters positioned at a distance z over the graphene monolayer. The emitter dipoles $\{\mathbf{d}_i\}_i$ are aligned to be perpendicular to the graphene layer and their magnitudes are quantified by the spontaneous emission rate γ_0 . The graphene is modeled as a two dimensional surface with conductivity $\sigma(E_f, \tau; \omega)$ [59] given in the local random phase approximation [39], where E_f is the Fermi energy tunable by gate doping and τ is the relaxation time accounting for the electron-phonon scattering (we use $\tau = 10^{-13}s$ [39]). The in-plane positions of the emitters are assumed to follow independent Gaussian distributions with width L . Our results thus depend on the set of parameters $N, L, z, E_f, \omega_z, \gamma_0, \Delta$. To focus on the phase transitions associated with the plasmonic evanescent modes, we shall omit the weak coupling to the propagating modes [7, 10] in the following. This is

done by replacing the total dyadic Green's function by its ‘scattering’ part which contains the information of the graphene SP [56].

Fig. 2(a) shows the location of the phase transitions as a function of the ensemble size and number of emitters. It demonstrates that the SR phase favors higher emitter densities. We also find that the phase diagram changes only little due to inhomogeneous broadening: For $z = 20$ nm and $N=100$ the Normal-SG phase boundary shifts L downward by only about 60 nm for a broadening as large as $\Delta = 0.1$ eV (here and throughout, $\hbar = 1$).

Although smaller z implies stronger emitter-graphene SP couplings, Fig. 2(a) shows that when the emitters are moved from the $z = 40$ nm to $z = 20$ nm distance to the graphene, the Normal-SG phases and SG-SR phase boundaries shift downward, i.e., they occur for higher emitter densities. When z is decreased, there is a complicated interplay between the enhanced SP-induced energy shift, see Fig. 2(b), leading to the Dicke SR phase, and the increased damping of the emitters, due to the same coupling, see Fig. 2(c). The competition between these effects is the main cause for the shift in the phase-transition boundaries. We note, however, for extremely small z , emitter-graphene bound states may form [60–64] so that different behavior, including polarization of the emitters, should be expected.

One may try to understand the SR phase of our system by comparing it with the Dicke model of a single cavity mode, where the effective emitter-emitter cou-

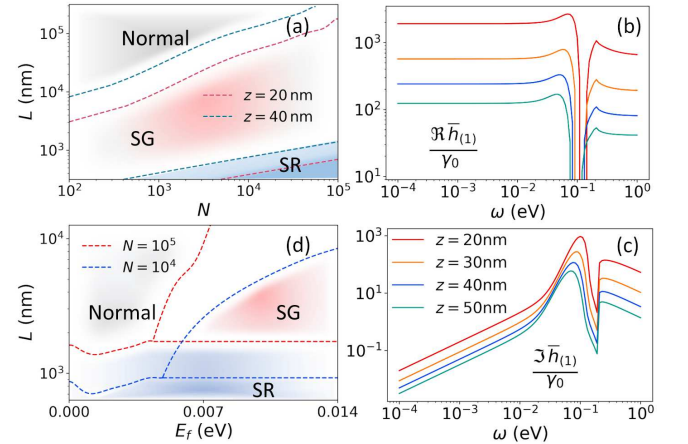


Figure 2. Results for systems with $\omega_z = 0.5$ eV and $E_f = 0.1$ eV: Panel (a) shows the $N - L$ phase diagram for $\gamma_0 = 10^{-5}$ eV, with different Normal-SG and SG-SR boundaries for $z = 20$ nm (red, lower dashed curves) and 40 nm (green, upper dashed curves); Panel (b) shows the value of $\Re \bar{h}_{(1)}(\omega)$, the energy shift induced by graphene, and panel (c) shows the value of $\Im \bar{h}_{(1)}(\omega)$, the graphene-induced emitter damping, as functions of frequency and different heights, $z = 20$ nm (red, top), 30 nm (orange), 40 nm (blue), 50 nm (green, bottom); Panel (d) shows the $E_f - L$ phase diagram for $z = 50$ nm, $\gamma_0 = 10^{-8}$ eV, with different Normal-SG and SG-SR boundaries for $N = 10^4$ (blue, lower dashed curves) and 10^5 (red, upper dashed curves).

pling Hamiltonian is given by $H_{eff} = -\sum_{i,j} J \sigma_i^x \cdot \sigma_j^x$, $J = g^2 \omega_c / (\omega_c^2 - \omega^2)$ [21], and the SR phase is reached when $g^2 N > \omega_z \omega_c / 4$. In our model, $\Re h_{ij}(\omega)$ plays the role of J and the mean $\Re \bar{h}_{(2)}(\omega)$ does not meet the equivalent SR criterion. However, smaller size sub-ensembles of emitters might experience strong enough mutual coupling. This fact is indicated by the large fluctuations of $\Re h_{ij}(\omega)$ resulting from the disorders, which are shown in Fig. 1F(e-f) of Ref. [56]. Such sub-ensembles would contribute significantly to the averaged polarization ψ_c of the system of emitters and lead to the SR phase. To properly account for the role of such sub-ensembles, a more refined description than the current mean-field approach will be required. A similar, so far un-noticed, relaxation of the SR criterion on the average coupling strength occurs for the Dicke model with a multi-mode cavity [21].

In the following we discuss the effect of tuning the Fermi energy E_f , a possibility unique to graphene. The SG-SR phase boundary is insensitive to E_f [56]. A higher E_f , however, leads to stronger graphene SP-induced emitter-emitter coupling [39, 40] and facilitates the Normal-SG phase transition as shown in the phase diagram of Fig. 2(d). It also shows a triple point and the Normal-SR phase boundary which are absent in Fig. 2(a). However, there is also a subtle SR \rightarrow Normal \rightarrow SR transition with an increasing E_f .

To understand it, we borrow ideas from the studies of spin-boson models [41–43], which suggest that the following three quantities might be pertinent: the emitter spectral response yield from the emitter linear susceptibility, $A^{SR}(\omega) = -2\Im Q_{cq}$; the spectral density $\Im \bar{h}_{(1)}(\omega)$

and the ‘many spin’ extension of the spectral density, $\Im \bar{h}_{(2)}(\omega)$. The spectral density is the central concept of models where a single spin couples to a continuum of bosons [41]. We note that only $A^{SR}(\omega)$ depends on ω_z [21] while $\Im \bar{h}_{(1)}(\omega)$ and $\Im \bar{h}_{(2)}(\omega)$ depend on the magnitude of the emitter dipoles quantified by γ_0/ω_z^3 .

To look closer at the Normal-SR transition, we depict an $E_f - \omega_z$ phase diagram in Fig. 3, for different values of γ_0/ω_z^3 . The frequency dependence of A^{SR} , $\Im \bar{h}_{(1)}$ and $\Im \bar{h}_{(2)}$ are shown in Fig. 3 for the four different Fermi energies $E_f = 0.1, 0.032, 0.004, 0.001$ eV. There are gaps between the positions of the peaks of $\Im \bar{h}_{(1)}(\omega)$ and those of $\Im \bar{h}_{(2)}(\omega)$, because the ‘short-range’ modes, important for self-interaction term $\Im \bar{h}_{(1)}(\omega)$, cannot propagate far enough to affect the averaged emitter-emitter coupling. Changing E_f shifts the peaks of A^{SR} , $\Im \bar{h}_{(1)}$ and $\Im \bar{h}_{(2)}$, and we observe a closer overlap of $A^{SR}(\omega)$ with $\Im \bar{h}_{(1)}(\omega)$, reflecting the influence of the SP-induced atomic decay, when the system is closer to the regime of the Normal phase. For the number of emitters N applied here, $\Im \bar{h}_{(1)}(\omega)$ and $N\Im \bar{h}_{(2)}(\omega)$ are comparable and suggest that the subtle E_f -dependence of the phase transition observed in Fig. 2(d) and Fig. 3 is a finite- N effect relevant to the graphene SP-induced emitter decay.

Additionally, the peaks of A^{SR} and $\Im \bar{h}_{(1,2)}$ shown in Fig. 3 generally occur far from the emitter resonance ω_z . This indicates that the influence of the inhomogeneous broadening, which scales as $(\Delta \frac{\omega \omega'}{\omega_z^2})^2$, is small. Moreover, their marked frequency dependence invalidates the Markov approximation, which would replace $\Im \bar{h}_{1,2}(\omega)$ by a constant taken at the atomic transition energy [63–66]. Indeed, our formalism considers the full spectral dependencies and does not apply the Markov approximation.

Summary and Outlook- To summarize, applying the Keldysh functional-integral approach, we have studied the Dicke phase transitions between the superradiant phase, spin-glass phase and the normal phase in a disordered emitter-graphene surface plasmon system. Our formalism is a generalization of the spin-boson model [41] to the many-spin system and is valid for general plasmonic systems. The variety of nanoscale plasmonic systems, and especially 2D materials like the graphene monolayer, constitute excellent platforms to test the fundamental collective phenomena of the Dicke model, and its effects in quantum optics, non-equilibrium dynamics of driven dissipative system, and condensed matter physics.

The superradiant phase is characterized by the emitter polarization. The spin-glass phase behaves differently from the superradiant phase at the low frequency regime of the emitter spectral response $-2\Im Q_{cq}(\omega)$ [22–24]. Thus they may be distinguished by observing their radio-frequency spectral response [67, 68]. Here we considered only the plasmonic evanescent modes, and disregarded weakly coupled optical scattering modes from the analysis. By employing an optical cavity, it may be possible to observe a hybrid coupling of the emitters to both surface plasmons and a cavity mode, and to use the cav-

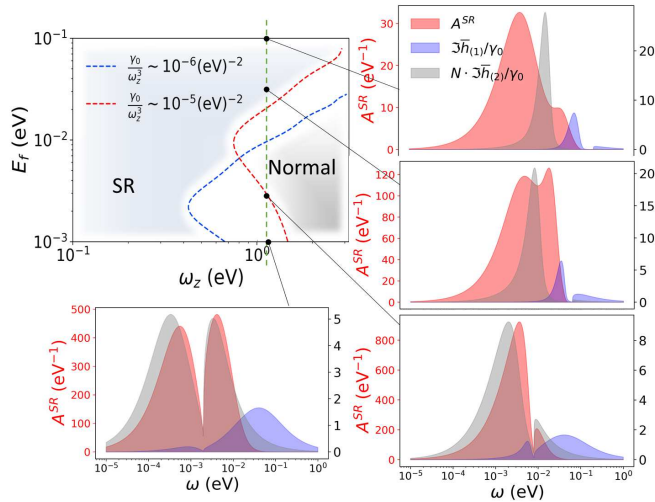


Figure 3. $E_f - \omega_z$ phase diagram for a system with $z = 50$ nm, $L = 10^3$ nm, $N = 2 \times 10^4$, and two different values of γ_0/ω_z^3 , so that when $\omega_z = 0.5$ eV, $\gamma_0 = 10^{-7}$ (blue dashed) or 10^{-6} eV (red dashed). For the case of $\omega_z = 1$ eV, the spectral densities $A^{SR} = -2\Im Q_{cq}(\omega)$ (red shaded), $\Im \bar{h}_{(1)}$ (grey shaded) and $\Im \bar{h}_{(2)}$ (blue shaded) are shown for different Fermi-energies, $E_f = 0.1, 0.032, 0.004, 0.001$ eV. The values of $\Im \bar{h}_{(1,2)}$ are shown on the right hand vertical axes.

ity response and transmission spectrum, as a signature of the surface plasmon Dicke phase transition [18, 23].

Acknowledgement- We sincerely thank Frank Koppens, Klass-Jan Tielrooij, Daniel Cano Reol, and Darrick

Chang for useful discussions and suggestions. This work was supported by European Unions Horizon 2020 research and innovation program (No. 712721, NanoQtech) and the Villum Foundation.

-
- [1] R. H. Dicke, Phys. Rev. **93**, 99 (1954).
 - [2] K. Hepp and E. H. Lieb, Annals of Physics **76**, 360 (1973).
 - [3] Y. K. Wang and F. T. Hioe, Phys. Rev. A **7**, 831 (1973).
 - [4] V. Emeljanov and Y. Klimontovich, Physics Letters A **59**, 366 (1976).
 - [5] K. Gawędzki and K. Rzażewski, Phys. Rev. A **23**, 2134 (1981).
 - [6] M. Bamba and T. Ogawa, Phys. Rev. A **90**, 063825 (2014).
 - [7] J. Keeling, Journal of Physics: Condensed Matter **19**, 295213 (2007).
 - [8] A. Vukics and P. Domokos, Phys. Rev. A **86**, 053807 (2012).
 - [9] A. Vukics, T. Grieser, and P. Domokos, Phys. Rev. Lett. **112**, 073601 (2014).
 - [10] A. Vukics, T. Grieser, and P. Domokos, Phys. Rev. A **92**, 043835 (2015).
 - [11] T. Grieser, A. Vukics, and P. Domokos, Phys. Rev. A **94**, 033815 (2016).
 - [12] K. Baumann, C. Guerlin, F. Brennecke, and T. Esslinger, Nature **464**, 1301 (2010).
 - [13] K. Baumann, R. Mottl, F. Brennecke, and T. Esslinger, Phys. Rev. Lett. **107**, 140402 (2011).
 - [14] F. Brennecke, R. Mottl, K. Baumann, R. Landig, T. Donner, and T. Esslinger, Proceedings of the National Academy of Sciences **110**, 11763 (2013).
 - [15] M. P. Baden, K. J. Arnold, A. L. Grimsom, S. Parkins, and M. D. Barrett, Phys. Rev. Lett. **113**, 020408 (2014).
 - [16] J. Klinder, H. Keßler, M. Wolke, L. Mathey, and A. Hemmerich, Proceedings of the National Academy of Sciences **112**, 3290 (2015).
 - [17] Z. Zhiqiang, C. H. Lee, R. Kumar, K. J. Arnold, S. J. Masson, A. S. Parkins, and M. D. Barrett, Optica **4**, 424 (2017).
 - [18] F. Dimer, B. Estienne, A. S. Parkins, and H. J. Carmichael, Phys. Rev. A **75**, 013804 (2007).
 - [19] D. Tolkunov and D. Solenov, Phys. Rev. B **75**, 024402 (2007).
 - [20] S. Gopalakrishnan, B. L. Lev, and P. M. Goldbart, Phys. Rev. Lett. **107**, 277201 (2011).
 - [21] P. Strack and S. Sachdev, Phys. Rev. Lett. **107**, 277202 (2011).
 - [22] L. M. Sieberer, M. Buchhold, and S. Diehl, Reports on Progress in Physics **79**, 096001 (2016).
 - [23] M. Buchhold, P. Strack, S. Sachdev, and S. Diehl, Phys. Rev. A **87**, 063622 (2013).
 - [24] E. G. D. Torre, S. Diehl, M. D. Lukin, S. Sachdev, and P. Strack, Phys. Rev. A **87**, 023831 (2013).
 - [25] P. Kirton and J. Keeling, Phys. Rev. Lett. **118**, 123602 (2017).
 - [26] V. M. Bastidas, C. Emary, B. Regler, and T. Brandes, Phys. Rev. Lett. **108**, 043003 (2012).
 - [27] O. Viehmann, J. von Delft, and F. Marquardt, Phys. Rev. Lett. **107**, 113602 (2011).
 - [28] M. Bamba, K. Inomata, and Y. Nakamura, Phys. Rev. Lett. **117**, 173601 (2016).
 - [29] L. J. Zou, D. Marcos, S. Diehl, S. Putz, J. Schmiedmayer, J. Majer, and P. Rabl, Phys. Rev. Lett. **113**, 023603 (2014).
 - [30] N. Lambert, C. Emary, and T. Brandes, Phys. Rev. Lett. **92**, 073602 (2004).
 - [31] C. Emary and T. Brandes, Phys. Rev. Lett. **90**, 044101 (2003).
 - [32] V. N. Pustovit and T. V. Shahbazy, Phys. Rev. Lett. **102**, 077401 (2009).
 - [33] M. S. Tame, K. R. McEnery, K. Özdemir, J. Lee, S. A. Maier, and M. S. Kim, Nature Physics **9**, 329 (2013).
 - [34] P. Törmä and W. L. Barnes, Reports on Progress in Physics **78**, 013901 (2015).
 - [35] D. E. Chang, A. S. Sørensen, P. R. Hemmer, and M. D. Lukin, Phys. Rev. Lett. **97**, 053002 (2006).
 - [36] W. Zhang, A. O. Govorov, and G. W. Bryant, Phys. Rev. Lett. **97**, 146804 (2006).
 - [37] D. N. Basov, M. M. Fogler, and F. J. García de Abajo, Science **354** (2016).
 - [38] A. N. Grigorenko, M. Polini, and K. S. Novoselov, Nature Photonics **6**, 749 (2012).
 - [39] F. H. L. Koppens, D. E. Chang, and F. J. Garca de Abajo, Nano Letters **11**, 3370 (2011).
 - [40] K. J. Tielrooij, L. Orona, A. Ferrier, M. Badioli, G. Navickaite, S. Coop, S. Nanot, B. Kalinic, T. Cesca, L. Gaudreau, Q. Ma, A. Centeno, A. Pesquera, A. Zurutuza, H. de Riedmatten, P. Goldner, F. J. García de Abajo, P. Jarillo-Herrero, and F. H. L. Koppens, Nature Physics **11**, 281 (2015).
 - [41] A. J. Leggett, S. Chakravarty, A. T. Dorsey, M. P. A. Fisher, A. Garg, and W. Zwerger, Rev. Mod. Phys. **59**, 1 (1987).
 - [42] P. P. Orth, D. Roosen, W. Hofstetter, and K. Le Hur, Phys. Rev. B **82**, 144423 (2010).
 - [43] A. Winter and H. Rieger, Phys. Rev. B **90**, 224401 (2014).
 - [44] B. Huttner and S. M. Barnett, Phys. Rev. A **46**, 4306 (1992).
 - [45] A. Drezet, Phys. Rev. A **95**, 023831 (2017).
 - [46] T. G. Philbin, New Journal of Physics **12**, 123008 (2010).
 - [47] T. Gruner and D.-G. Welsch, Phys. Rev. A **53**, 1818 (1996).
 - [48] H. T. Dung, L. Knöll, and D.-G. Welsch, Phys. Rev. A **57**, 3931 (1998).
 - [49] S. F. Edwards and P. W. Anderson, Journal of Physics F: Metal Physics **5**, 965 (1975).
 - [50] D. Dzsojtjan, A. S. Sørensen, and M. Fleischhauer, Phys. Rev. B **82**, 075427 (2010).
 - [51] J. B. Kogut, Rev. Mod. Phys. **51**, 659 (1979).
 - [52] J. Ye, S. Sachdev, and N. Read, Phys. Rev. Lett. **70**, 4011 (1993).
 - [53] M. P. Kennett, C. Chamon, and J. Ye, Phys. Rev. B **64**, 224408 (2001).

- [54] S. Sachdev, Quantum phase transitions, (Cambridge University Press, 2011) Chap. 5.5.3, 2nd ed.
- [55] H. Aoki, N. Tsuji, M. Eckstein, M. Kollar, T. Oka, and P. Werner, Rev. Mod. Phys. **86**, 779 (2014).
- [56] Supplemental Material.
- [57] K. H. Fischer and J. A. Hertz, Spin Glasses, reprint edition ed., Cambridge Studies in Magnetism (Book 1) (Cambridge University Press, 1993).
- [58] H. Goto and K. Ichimura, Phys. Rev. A **77**, 053811 (2008).
- [59] G. W. Hanson, J. Appl. Phys. **103**, 064302 (2008).
- [60] Q.-J. Tong, J.-H. An, H.-G. Luo, and C. H. Oh, Phys. Rev. A **81**, 052330 (2010).
- [61] C.-J. Yang and J.-H. An, Phys. Rev. B **95**, 161408 (2017).
- [62] I. Thanopoulos, V. Yannopoulos, and E. Paspalakis, Phys. Rev. B **95**, 075412 (2017).
- [63] A. González-Tudela, P. A. Huidobro, L. Martín-Moreno, C. Tejedor, and F. J. García-Vidal, Phys. Rev. B **89**, 041402 (2014).
- [64] A. González-Tudela, F. J. Rodríguez, L. Quiroga, and C. Tejedor, Phys. Rev. B **82**, 115334 (2010).
- [65] H. T. Dung, L. Knöll, and D.-G. Welsch, Phys. Rev. A **66**, 063810 (2002).
- [66] I. de Vega and D. Alonso, Rev. Mod. Phys. **89**, 015001 (2017).
- [67] J. T. Stewart, J. P. Gaebler, and D. S. Jin, Nature **454**, 744 (2008).
- [68] R. Haussmann, M. Punk, and W. Zwerger, Phys. Rev. A **80**, 063612 (2009).
- [69] R. L. Stratonovich, Soviet Physics Doklady **2**, 416 (1957).
- [70] J. Hubbard, Phys. Rev. Lett. **3**, 77 (1959).

I. SUPPLEMENTAL MATERIAL

In this supplemental material, we shall present details of our derivations of the Dicke phase transitions based on the Keldysh functional-integral approach. The Keldysh action of a system with Hamiltonian H and Lindblad dissipation operator $\{L_\alpha\}$ is formulated, by representing the dynamical variables by ψ , according to [22]

$$S = \int dt \left[\psi_+^* i \partial_t \psi_+ - \psi_- i \partial_t \psi_- - (H_+ - H_-) - i \sum_\alpha \gamma_\alpha (L_{\alpha+} L_{\alpha-}^* - \frac{1}{2} L_{\alpha+}^* L_{\alpha+} - \frac{1}{2} L_{\alpha-}^* L_{\alpha-}) \right]. \quad (\text{I.11})$$

We employ two sets of bosonic variables, ϕ_i for the emitters and $\mathbf{f}(\mathbf{r}', \tilde{\omega})$ for the electromagnetic environment.

This Supplemental Material includes the following contents:

IA: The Keldysh action of the free emitters;

IB: The Keldysh action of the SP field, emitter-field coupling, and effective emitter-emitter coupling mediated by the graphene SP field;

IC: Averaging over the disorders;

ID: Determining the phases by the saddle point equations;

IE: The treatment of inhomogeneous broadening;

IF: Some notes about the calculation of the emitter-graphene surface plasmons system, including curves of the averaged coupling strength and the covariance matrix elements.

A. Action of the Free Emitters

The Keldysh action for the free emitters is given as Eq. (4) in the main text and is derived from Eq. (I.11) with the mapping

$$\sigma_i^x(t) \rightarrow \phi_i(t), \quad \sigma_i^z(t) \rightarrow \frac{2}{\omega_z^2} (\partial_t \phi_i)^2 - 1. \quad (\text{I.12})$$

where we have omitted the effect of inhomogeneous broadening. Discussion on that is deferred to Sec. IE. Then we substitute $\phi_i(t)$ into Eq. (I.11). Since $\phi_i(t)$ is a real variable, the first two terms of Eq. (I.11) are time-derivative terms, that is, $\phi_\pm^* i \partial_t \phi_\pm = \phi_\pm i \partial_t \phi_\pm = \frac{1}{2} i \partial_t (\phi_\pm^2)$. These terms are negligible because they have no effects on the action after the integral over time.

The restriction $\phi_\pm^2(t) = 1$ is imposed by multiplying the Keldysh partition function by the delta functions $\prod_t \delta(\phi_\pm^2(t) - 1)$. This process brings Lagrange multipliers $\lambda_\pm(t)$ to the action according to the relation that:

$$\prod_t \delta(\phi_\pm^2(t) - 1) = \int D\lambda_\pm(t) e^{i \int dt \lambda_\pm(t) (\phi_\pm^2(t) - 1)}. \quad (\text{I.13})$$

Then, we perform the Keldysh rotation, a unitary transformation of the contour index:

$$\begin{aligned} \phi_c &= \frac{1}{\sqrt{2}} (\phi_+ + \phi_-), & \phi_q &= \frac{1}{\sqrt{2}} (\phi_+ - \phi_-), \\ \lambda_c &= \lambda_+ + \lambda_-, & \lambda_q &= \lambda_+ - \lambda_-. \end{aligned} \quad (\text{I.14})$$

where the subscripts 'c' and 'q' stand for 'classical' and 'quantum', respectively [22]. The constraint equation then amounts to inclusion of the Lagrange multiplier term

$$2 \int_t \lambda_c(t) \phi_c(t) \phi_q(t) + \lambda_q(t) (\phi_c^2(t) + \phi_q^2(t) - 2), \quad (\text{I.15})$$

into the action, where \int_t is shorthand for $\int dt$. Retaining only its static contribution, we use the ansatz that

$$\lambda_{i,\alpha}(\omega) = 2\pi \lambda_{i,\alpha} \delta(\omega) \quad (\text{I.16})$$

in the Fourier domain, where $\alpha \in \{c, q\}$. Finally, the Keldysh action of the free emitters is written as

$$\begin{aligned} S_e &= \sum_{i=1}^N \int_w (\phi_{i,c}, \phi_{i,q})_{-\omega} \begin{pmatrix} \lambda_{i,q} & \lambda_{i,c} - \frac{\omega^2}{\omega_z} \\ \lambda_{i,c} - \frac{\omega^2}{\omega_z} & \lambda_{i,q} \end{pmatrix} \begin{pmatrix} \phi_{i,c} \\ \phi_{i,q} \end{pmatrix}_\omega \\ &\quad - 2 \sum_{i=1}^N \lambda_{i,q} 2\pi \delta(0), \end{aligned} \quad (\text{I.17})$$

where \int_w is shorthand for $\int \frac{d\omega}{2\pi}$.

B. Action for the Plasmonic Environment

The plasmonic electromagnetic environment is quantized through the complex field $\mathbf{f}(\mathbf{r}', \tilde{\omega})$. Here we denote it as $f_{a,\mathbf{r},\tilde{\omega}}$, where “ a ” labels the three Cartesian directions. The Keldysh action of the free plasmonic environment and its coupling to the emitters is

$$S_{f,ef} = \sum_a \int_{\tilde{\omega}, \mathbf{r}', \omega} (f_{a,\mathbf{r},\tilde{\omega};c}^* \ f_{a,\mathbf{r},\tilde{\omega};q})_{\omega} D_{\tilde{\omega}}(\omega) \begin{pmatrix} f_{a,\mathbf{r},\tilde{\omega};c} \\ f_{a,\mathbf{r},\tilde{\omega};q} \end{pmatrix}_{\omega} \\ - \sum_{i=1}^N \sum_a \int_{\tilde{\omega}, \mathbf{r}', \omega} g_{ia}(\mathbf{r}', \tilde{\omega}) \left(\phi_{i,-\omega;c} f_{a,\mathbf{r}',\tilde{\omega};q}(\omega) \right. \\ \left. + \phi_{i,-\omega;q} f_{a,\mathbf{r},\tilde{\omega};c}(\omega) \right) + g_{ia}^*(\mathbf{r}', \tilde{\omega}) \left(\phi_{i,\omega;c} f_{a,\mathbf{r}',\tilde{\omega};q}^*(\omega) \right. \\ \left. + \phi_{i,\omega;q} f_{a,\mathbf{r},\tilde{\omega};c}^*(\omega) \right), \quad (\text{I.18})$$

where $\int_{\tilde{\omega}}$ is shorthand for $\int_0^{\infty} \frac{d\tilde{\omega}}{2\pi}$, $\int_{\mathbf{r}'}$ is shorthand for $\int d^3\mathbf{r}'$, and the matrix $D_{\tilde{\omega}}(\omega)$ is defined as

$$D_{\tilde{\omega}}(\omega) = \begin{pmatrix} 0 & \omega - \tilde{\omega} - i\epsilon \\ \omega - \tilde{\omega} + i\epsilon & 2i\epsilon \end{pmatrix}, \quad (\text{I.19})$$

and ϵ stands for an infinitesimal positive constant; the coupling strength is

$$g_{ia}(\mathbf{r}', \tilde{\omega}) = -i \sqrt{\frac{\epsilon_I(\mathbf{r}', \tilde{\omega})}{\hbar\pi\epsilon_0}} \frac{\tilde{\omega}^2}{c^2} \sum_b \mathbf{d}_{ib} \mathbf{G}_{ba}(\mathbf{r}_i, \mathbf{r}', \tilde{\omega}). \quad (\text{I.20})$$

In Eq. (I.18) all terms with identical indices of $\tilde{\omega}$ and ω share the same matrix $D_{\tilde{\omega}}(\omega)$. Therefore, after integrating out the field of $\mathbf{f}(\mathbf{r}, \tilde{\omega})$, $S_{f,ef}$ turns out to be an effective emitter-emitter coupling action:

$$S_{ee}^{(p)} = - \sum_{i,j=1}^N \int_{\tilde{\omega}, \omega} \tilde{g}_{ij}(\tilde{\omega}) (\phi_{i,c} \ \phi_{j,q})_{-\omega} \\ \times \sigma_x D_{\tilde{\omega}}^{-1} \sigma_x \begin{pmatrix} \phi_{j,c} \\ \phi_{j,q} \end{pmatrix}_{\omega}, \quad (\text{I.21})$$

where the coupling strength $\tilde{g}_{ij}(\tilde{\omega})$ is

$$\tilde{g}_{ij}(\tilde{\omega}) = \sum_a \int_{\mathbf{r}'} g_{ia}(\mathbf{r}', \tilde{\omega}) g_{ja}^*(\mathbf{r}', \tilde{\omega}) \\ = \frac{1}{\pi\epsilon_0\hbar c^2} \tilde{\omega}^2 \mathbf{d}_i \cdot \Im \mathbf{G}(\mathbf{r}_i, \mathbf{r}_j, \tilde{\omega}) \cdot \mathbf{d}_j, \quad (\text{I.22})$$

and σ_x is the matrix $\begin{pmatrix} 0 & 1 \\ 1 & 0 \end{pmatrix}$. In the derivation of \tilde{g}_{ij} , we have used the relation

$$\sum_b \frac{\omega^2}{c^2} \int_{\mathbf{r}'} \epsilon_I(\mathbf{r}', \omega) \mathbf{G}_{ab}(\mathbf{r}_i, \mathbf{r}', \omega) \mathbf{G}_{cb}^*(\mathbf{r}_j, \mathbf{r}', \omega) \\ = \Im \mathbf{G}_{ac}(\mathbf{r}_i, \mathbf{r}_j, \omega). \quad (\text{I.23})$$

The inverse of $D_{\tilde{\omega}}(\omega)$ is expressed as

$$D_{\tilde{\omega}}^{-1}(\omega) = \begin{pmatrix} \frac{-2i\epsilon}{(\omega - \tilde{\omega})^2 + \epsilon^2} & \frac{1}{\omega - \tilde{\omega} + i\epsilon} \\ \frac{1}{\omega - \tilde{\omega} - i\epsilon} & 0 \end{pmatrix}. \quad (\text{I.24})$$

Then, using the relations

$$\lim_{\epsilon \rightarrow 0^+} \frac{\epsilon}{(\omega - \omega_{\mu})^2 + \epsilon^2} = \pi \delta(\omega - \omega_{\mu}), \\ \lim_{\epsilon \rightarrow 0^+} \frac{1}{\omega - \omega_{\mu} \pm i\epsilon} = \mathcal{P} \frac{1}{\omega - \omega_{\mu}} \mp i\pi \delta(\omega - \omega_{\mu}), \quad (\text{I.25})$$

we can implement the integral of $\tilde{\omega}$ in $S_{ee}^{(p)}$, i.e.,

$$\Lambda(\omega) = \int_{\tilde{\omega}} \tilde{g}_{ij}(\tilde{\omega}) \sigma_x D_{\tilde{\omega}}^{-1}(\omega) \sigma_x. \quad (\text{I.26})$$

The result is

$$\Lambda(\omega) = \begin{pmatrix} 0 & F_{ij}(\omega) + i\pi \Delta_{ij}(\omega) \\ F_{ij}(\omega) - i\pi \Delta_{ij}(\omega) & -2i\pi \Delta_{ij}(\omega) \end{pmatrix}, \quad (\text{I.27})$$

where the elements of the matrix are

$$F_{ij}(\omega) = \int_{\tilde{\omega}} \frac{\tilde{\omega}^2}{\pi\epsilon_0\hbar c^2} \mathbf{d}_i \cdot \Im \mathbf{G}(\mathbf{r}_i, \mathbf{r}_j, \tilde{\omega}) \cdot \mathbf{d}_j \mathcal{P} \frac{1}{\omega - \tilde{\omega}}, \quad (\text{I.28a})$$

$$\Delta_{ij}(\omega) = \int_{\tilde{\omega}} \frac{\tilde{\omega}^2}{\pi\epsilon_0\hbar c^2} \mathbf{d}_i \cdot \Im \mathbf{G}(\mathbf{r}_i, \mathbf{r}_j, \tilde{\omega}) \cdot \mathbf{d}_j \delta(\omega - \tilde{\omega}). \quad (\text{I.28b})$$

Due to the symmetry of the indices, we reshape $\Lambda(\omega)$ by

$$\Lambda(\omega) \rightarrow \frac{1}{2} \left[\Lambda(\omega) + \Lambda^T(-\omega) \right], \quad (\text{I.29})$$

where “ T ” stands for matrix transposition. Then the elements of $\Lambda(\omega)$ are modified to

$$\Lambda_{22} \rightarrow -i\pi (\Delta_{ij}(\omega) + \Delta_{ij}(-\omega)) \\ = \frac{-i\omega^2}{\hbar\epsilon_0 c^2} \mathbf{d}_i \cdot \Im \mathbf{G}(\mathbf{r}_i, \mathbf{r}_j, |\omega|) \cdot \mathbf{d}_j \\ = \text{sign}(\omega) \frac{-i\omega^2}{\hbar\epsilon_0 c^2} \mathbf{d}_i \cdot \Im \mathbf{G}(\mathbf{r}_i, \mathbf{r}_j, \omega) \cdot \mathbf{d}_j, \quad (\text{I.30})$$

where we have used the relation $\mathbf{G}(\omega) = \mathbf{G}^*(-\omega)$, and

$$\Lambda_{21} \rightarrow \frac{1}{2} \left(F_{ij}(\omega) + i\pi \Delta_{ij}(\omega) + F_{ij}(-\omega) - i\pi \Delta_{ij}(-\omega) \right). \quad (\text{I.31})$$

To evaluate the expressions, we shall use the Kramers-Kronig relation. For a function $\chi(\omega)$ which is analytic in the closed upper half-plane of ω and vanishes like $1/|\omega|$ or faster as $|\omega| \rightarrow \infty$, and $\chi(\omega) = \chi^*(-\omega)$, we have

$$\Re \chi(\omega) = \frac{2}{\pi} \int_0^{\infty} d\omega' \mathcal{P} \frac{\omega' \Im \chi(\omega')}{\omega'^2 - \omega^2}. \quad (\text{I.32})$$

Applying this to $\omega^2 \mathbf{G}(\omega)$, we obtain

$$F_{ij}(\omega) + F_{ij}(-\omega) = \frac{-\omega^2}{\hbar\epsilon_0 c^2} \mathbf{d}_i \cdot \Re \mathbf{G}(\mathbf{r}_i, \mathbf{r}_j, \omega) \cdot \mathbf{d}_j, \quad (\text{I.33})$$

which finally gives

$$\Lambda_{21} \rightarrow \frac{-\omega^2}{2\hbar\epsilon_0 c^2} \mathbf{d}_i \cdot \mathbf{G}(\mathbf{r}_i, \mathbf{r}_j, \omega) \cdot \mathbf{d}_j \equiv -h_{ij}, \quad (\text{I.34a})$$

$$\Lambda_{12} \rightarrow \frac{-\omega^2}{2\hbar\epsilon_0 c^2} \mathbf{d}_i \cdot \mathbf{G}^*(\mathbf{r}_i, \mathbf{r}_j, \omega) \cdot \mathbf{d}_j = -h_{ij}^*. \quad (\text{I.34b})$$

Together with $\Lambda_{11} = 0$, this yields the graphene-induced emitter-emitter coupling action $S_{ee}^{(p)}$ given in Eq. (5) in the main text:

$$S_{ee}^{(p)} = \sum_{i,j=1}^N \int_{-\infty}^{\infty} \frac{d\omega}{2\pi} (\phi_{i,c} \ \phi_{i,q})_{-\omega} \quad (\text{I.35a})$$

$$\times \begin{pmatrix} 0 & h_{ij}^*(\omega) \\ h_{ij}(\omega) & 2i\Im h_{ij}(|\omega|) \end{pmatrix} \begin{pmatrix} \phi_{j,c} \\ \phi_{j,q} \end{pmatrix}_{\omega}$$

$$h_{ij}(\omega) = \frac{\omega^2}{2\hbar\epsilon_0 c^2} \mathbf{d}_i \cdot \mathbf{G}(\mathbf{r}_i, \mathbf{r}_j, \omega) \cdot \mathbf{d}_j. \quad (\text{I.35b})$$

Note that the derivation of $S_{ee}^{(p)}$ does not discard counter-rotating-wave terms nor apply the Markov approximation, which treats the ω -dependence of the spectrum as a constant.

C. Spatial Disorder

We define two matrices

$$V^1 = \sigma^x = \begin{pmatrix} 0 & 1 \\ 1 & 0 \end{pmatrix}, \quad V^2 = i \begin{pmatrix} 0 & -1 \\ 1 & 2\text{sign}(\omega) \end{pmatrix}. \quad (\text{I.36})$$

Then, $S_{ee}^{(p)}$ can be brought to the form

$$S_{ee}^{(p)} = \sum_{i,j=1}^N \int_{\omega} \Re h_{ij}(\omega) v_{ij}^{(1)}(\omega) + \Im h_{ij}(\omega) v_{ij}^{(2)}(\omega), \quad (\text{I.37})$$

where

$$v_{ij}^{(a)}(\omega) = (\phi_{i,c} \ \phi_{i,q})_{-\omega} \cdot V^a \cdot \begin{pmatrix} \phi_{j,c} \\ \phi_{j,q} \end{pmatrix}_{\omega}. \quad (\text{I.38})$$

This form will facilitate the Gaussian averaging over the coupling strengths $\Re h_{ij}(\omega)$, $\Im h_{ij}(\omega)$. For terms with subscript $i \neq j$, we assume a multi-component Gaussian distribution

$$\bar{h}_{(2)}(\omega) = \int d^3 \mathbf{r}_a d^3 \mathbf{r}_b p(\mathbf{r}_a, \mathbf{r}_b) h_{ab}(\omega), \quad (\text{I.39a})$$

$$M(\omega, \omega') = \int d^3 \mathbf{r}_a d^3 \mathbf{r}_b p(\mathbf{r}_a, \mathbf{r}_b) \times \begin{pmatrix} \delta \Re h_{ab}(\omega) \delta \Re h_{ab}(\omega') & \delta \Re h_{ab}(\omega) \delta \Im h_{ab}(\omega') \\ \delta \Im h_{ab}(\omega) \delta \Re h_{ab}(\omega') & \delta \Im h_{ab}(\omega) \delta \Im h_{ab}(\omega') \end{pmatrix}. \quad (\text{I.39b})$$

These are Eqs. (7a) and (7b) of the main text. Different from the emitter-emitter coupling strength, the values of the graphene-induced individual terms,

$\Re h_{ii}(\omega)$, $\Im h_{ii}(\omega)$, depend only on the distance from the emitter to the graphene. Since we have assumed that the layer of emitters is parallel to the graphene monolayer, all the $h_{ii}(\omega)$ are fixed and identical. In Sec. IF, we present figures showing these coupling strengths and the elements of the covariance matrix.

To explore the phase transition at $N \rightarrow \infty$, we define

$$h_i^d = N \times h_{ii}, \quad h^o = N \times \bar{h}_{(2)}, \quad M^o = N \times M, \quad (\text{I.40})$$

so that after averaging over h_{ij} ($i \neq j$) as described in the main text, we have

$$\begin{aligned} \bar{S}_{ee}^{(p)} = & \frac{1}{N} \sum_{i=1}^N \int_{\omega} (h_i^d - h^o)_a(\omega) v_{ii}^{(a)}(\omega) \\ & + \frac{1}{N} \sum_{i,j=1}^N \int_{\omega} h_a^o(\omega) v_{ij}^{(a)}(\omega) \\ & + i \frac{1}{N} \sum_{i \neq j=1}^N \int_{\omega, \omega'} v_{ij}^{(a)}(\omega) M_{ab}^o(\omega, \omega') v_{ij}^{(b)}(\omega'), \end{aligned} \quad (\text{I.41})$$

where the summation over replicated indices a, b are implicit assumed; and we have written $h^{d(o)}$ in the vector form of $(\Re h^{d(o)}, \Im h^{d(o)})$. While, in the third line of Eq. (I.41), terms with $i = j$ are excluded, in the limit of large N , we may release this exclusion (see more discussion in Sec. IE) and define

$$\begin{aligned} \Phi_{\alpha}(\omega) &= \sum_{i=1}^N \phi_{i,\alpha}(\omega), \\ \Phi_{\alpha\beta}(\omega, \omega') &= \sum_{i=1}^N \phi_{i,\alpha}(\omega) \phi_{i,\beta}(\omega'). \end{aligned} \quad (\text{I.42})$$

Now the Keldysh action can be expressed in terms of Φ_{α} and $\Phi_{\alpha\beta}$:

$$\begin{aligned} S = & \frac{1}{N} \sum_{i=1}^N \int_{\omega} \phi_{i,\alpha}(-\omega) \phi_{i,\beta}(\omega) \Lambda_{i,\alpha\beta}^e(\omega) - 2 \sum_{i=1}^N \lambda_{i,q} 2\pi \delta(0) \\ & + \frac{1}{N} \int_{\omega} \Phi_{\alpha}(-\omega) \Phi_{\beta}(\omega) \Lambda_{\alpha\beta}^{ce}(\omega) \\ & + i \frac{1}{N} \int_{\omega, \omega'} \Phi_{\alpha\beta}(-\omega, -\omega') \tilde{M}_{\alpha\beta, \alpha'\beta'}(\omega, \omega') \Phi_{\alpha'\beta'}(\omega, \omega'), \end{aligned} \quad (\text{I.43})$$

where the new matrixes are defined as

$$\begin{aligned} \Lambda_i^e &= N \begin{pmatrix} \lambda_{i,q} & \lambda_{i,c} - \frac{\omega^2}{\omega_i} \\ \lambda_{i,c} - \frac{\omega^2}{\omega_i} & \lambda_{i,q} \end{pmatrix} + (h_i^d - h^o)_a V^a, \\ \Lambda^{ce} &= h_a^o V^a, \\ \tilde{M}_{\alpha\beta, \alpha'\beta'}(\omega, \omega') &= \sum_{s,t} V_{\alpha\alpha'}^s(\omega) M_{st}^o(\omega, \omega') V_{\beta\beta'}^t(\omega'). \end{aligned} \quad (\text{I.44})$$

Then we apply the Hubbard-Stratonovich transformation [69, 70] based on the formula that

$$\begin{aligned} & \int D[\psi_\alpha] e^{-iN \int_\omega \psi_\alpha(-\omega) \Lambda_{\alpha\beta}^{ce}(\omega) \psi_\beta(\omega) - 2i \int_\omega \psi_\alpha(-\omega) \Lambda_{\alpha\beta}^{ce}(\omega) \phi_\beta(\omega)} \\ & \propto e^{i \frac{1}{N} \int_\omega \phi_\alpha(-\omega) \Lambda_{\alpha\beta}^{ce}(\omega) \phi_\beta(\omega)}, \end{aligned} \quad (\text{I.45})$$

The coefficient of proportionality in the above formula is a constant, which is irrelevant to the dynamical variables. The Hubbard-Stratonovich transformation of $\Phi_{\alpha\beta}$ is based on a similar formula of Gaussian integral

$$\begin{aligned} & \int D[Q_a] e^{-N \int_q Q_a(-q) \tilde{M}_{ab}(q) Q_b(q) - 2i \int_q Q_a(-q) \tilde{M}_{ab}(q) \Phi_b(q)} \\ & \propto e^{-\frac{1}{N} \int_q \Phi_a(-q) \tilde{M}_{ab}(q) \Phi_b(q)}, \end{aligned} \quad (\text{I.46})$$

where “a” and “b” denote the subscript $(\alpha\beta)$ and $(\alpha'\beta')$, and “q” is used to abbreviate (ω, ω') .

After the transformations, the Keldysh action has some residual ϕ_i terms of order less than or equal to two. We can eliminate these terms by Gaussian integrals.

Then the Keldysh action becomes a functional of the Lagrange multiplier $\lambda_{i,\alpha}$ and the two new dynamical variables, ψ_α and $Q_{\alpha\beta}$, which are introduced in Eq. (9) of the main text. Substituting the static ansatz at mean field level,

$$\begin{aligned} \psi_\alpha(\omega) &= 2\pi\psi_\alpha\delta(0), \\ Q_{\alpha\beta}(\omega, \omega') &= Q_{\alpha\beta}(\omega)2\pi\delta(\omega + \omega'), \end{aligned} \quad (\text{I.47})$$

this finally yields the action in terms of $\psi_\alpha, Q_{\alpha\beta}$ and λ_i

$$\begin{aligned} S &= \frac{i}{2} \sum_{i=1}^N \text{tr} \ln(2\mathbf{L}_i) - 2 \sum_{i=1}^N \pi\delta(0) (\Lambda^{ce}\psi)^T \mathbf{L}_i^{-1}(0) (\Lambda^{ce}\psi) \\ &+ i2\pi\delta(0)N \int_\omega Q_{\alpha\beta}(-\omega) \tilde{M}_{\alpha\beta, \alpha'\beta'}(\omega, -\omega) Q_{\alpha'\beta'}(\omega) \\ &- 2\pi\delta(0)N \psi_\alpha \Lambda_{\alpha\alpha'}^{ce}(0) \psi_{\alpha'} - 4\pi\delta(0) \sum_{i=1}^N \lambda_{i,q}. \end{aligned} \quad (\text{I.48})$$

where the matrix \mathbf{L}_i is defined as

$$\begin{aligned} \mathbf{L}_i(\omega, \omega') &= \mathbf{L}(\omega)2\pi\delta(\omega + \omega') \\ \mathbf{L}_{i, \alpha\beta}(\omega) &= \frac{1}{N} \Lambda_{i, \alpha\beta}^e(-\omega) - 2Q_{\alpha'\beta'}(-\omega) \tilde{M}_{\alpha'\beta', \alpha\beta}(\omega, -\omega). \end{aligned} \quad (\text{I.49})$$

D. Saddle Point Equations

We now turn to the solution of the saddle point equations

$$\frac{\delta}{\delta q} S \stackrel{!}{=} 0, \quad q \in \{\lambda_{i,\alpha}, \psi_\alpha, Q_{\alpha\beta}\}, \quad (\text{I.50})$$

which is restricted by the causality conditions $\lambda_q = Q_{qq} = \psi_q = 0$.

1. Equations for $\lambda_{i,\alpha}$

We assume $\lambda_{i,\alpha} = \lambda_\alpha$, and replace the summation in Eq. (I.48) with a factor of N. The saddle point equation with respect to the Lagrangian multiplier λ_q is

$$\begin{aligned} & \frac{i}{2} \int_\omega \text{tr}[\mathbf{L}_{reg}^{-1}(\omega)] - \frac{1}{\det \mathbf{L}(0)} \left(\psi_c^2 (\Lambda_{cq}^{ce})^2 \right. \\ & \left. + q_{EA} \tilde{M}_{cc,qq}(0) \right) - 2 = 0, \end{aligned} \quad (\text{I.51})$$

which confirms the restriction $\phi_i^2 = 1$. In Eq. (I.51), \mathbf{L}_{reg} refers to the part defined with Q_{cc}^{reg} . The equation with respect to the Lagrangian multiplier λ_c is

$$-\frac{i}{2} \int_\omega \frac{1}{\det \mathbf{L}(\omega)} \text{tr}[\sigma_x \mathbf{L}(\omega)] = 0. \quad (\text{I.52})$$

This equation is a statement of the universal property of the Keldysh Green's function that

$$Q^R(t, t) + Q^A(t, t) = 0, \quad (\text{I.53})$$

where $Q^R = Q_{cq}$ and $Q^A = Q_{qc}$.

2. Equations for ψ_α

For ψ_c , the saddle-point equation is trivial, because

$$(\Lambda^{ce})_{cc} = 0, (\Lambda^{ce} \mathbf{L}^{-1} \Lambda^{ce})_{cc} = 0, (\mathbf{L}^{-1})_{qq} = 0, \quad (\text{I.54})$$

when $\lambda_q = \psi_q = Q_{qq} = 0$.

For ψ_q , the saddle-point equation gives

$$\psi_c (\Lambda_{qc}^{ce} (\mathbf{L}^{-1})_{cq} + 1) = 0, \quad (\text{I.55})$$

which gauges the relation between λ_c and Q_{cq} , in the SR phase where $\psi_c \neq 0$.

3. Equations for $Q_{\alpha\beta}^{reg}$

The Edwards-Anderson order parameter q_{EA} is introduced as the singular part of $Q_{cc}(\omega)$:

$$Q_{cc}(\omega) = Q_{cc}^{reg}(\omega) - 2\pi i q_{EA} \delta(\omega), \quad (\text{I.56})$$

and the saddle point equation for the regular component reads

$$\begin{aligned} 2Q_{\alpha\beta}^{reg}(\omega) &= [\mathbf{L}(\omega)]_{reg, \beta\alpha}^{-1} + 4i\pi \left(\frac{\psi_c^2 (\Lambda_{cq}^{ce})^2}{\det \mathbf{L}(0)} \right. \\ & \left. + q_{EA} + q_{EA} \frac{\tilde{M}_{cc,qq}(0)}{\det \mathbf{L}(0)} \right) \delta_{\alpha c} \delta_{\beta c} \delta(\omega). \end{aligned} \quad (\text{I.57})$$

Note that, this equation can be separated into the regular part and the singular part at $\omega = 0$:

$$\begin{aligned} 2Q_{\alpha\beta}^{reg} &= [\mathbf{L}(\omega)]_{reg, \beta\alpha}^{-1}; \\ (\Lambda_{cq}^{ce})^2 \psi_c^2 &= -q_{EA} (\tilde{M}_{cc,qq} + \det \mathbf{L}(0)). \end{aligned} \quad (\text{I.58})$$

For the regular part, implementing the substitution of Eq. (I.49) for the cq component gives

$$\frac{1}{2Q_{cq}} = \lambda_c - \frac{\omega^2}{\omega_z} + \bar{h}_{(1)} - \bar{h}_{(2)} - 2Q_{cq}\tilde{M}_{qc,cq}(\omega, -\omega). \quad (\text{I.59})$$

where we have assumed $\lambda_{i,\alpha} = \lambda_\alpha$ for every emitter.

We find that this equation does not have a unique solution except in the absence of randomness, $M \rightarrow 0$, where the second line of Eq. (I.48) vanishes and the Keldysh action attains the value given in Ref. [24]. We select the solution that is continuously connected to the unique solution to Eq. (I.59) with $\tilde{M} = 0$, under the variation of $\lambda\tilde{M}, \lambda : 1 \rightarrow 0$.

The regular part of Q_{cc} turns out to be

$$Q_{cc}^{reg} = \frac{4|Q_{cq}|^2}{1 - 4|Q_{cq}|^2\tilde{M}_{cc,qq}(\omega, -\omega)} \left(Q_{qc}\tilde{M}_{cq,qq}(\omega, -\omega) + Q_{cq}\tilde{M}_{qc,qq}(\omega, -\omega) - i\text{sgn}(\omega)(\Im\bar{h}_{(1)} - \Im\bar{h}_{(2)}) \right). \quad (\text{I.60})$$

The causality condition of the Keldysh formalism implies $Q_{qq} = \lambda_{i,q} = \psi_q = 0$, and $Q_{cq}(\omega) = Q_{qc}^*(\omega)$ [22].

Since the Edward-Anderson order parameter q_{EA} is non-negative, it follows from the second equation of Eq. (I.58) that to have $\psi_c^2 > 0$, we must have

$$\tilde{M}_{cc,qq}(0, 0) + \det \mathbf{L}(0) < 0. \quad (\text{I.61})$$

This relation helps to distinguish the SR phase and the SG phase.

4. Determination of λ_c and the three phases

In the SR phase, $\psi_c \neq 0$, so that Eq. (I.55) determines the value of λ_c^{SR} :

$$\lambda_c^{SR} = -\bar{h}_{(1)}(0) + \bar{h}_{(2)}(0) - \Lambda_{qc} - \frac{N}{\Lambda_{qc}}M_{11}(0, 0), \quad (\text{I.62})$$

where M_{11} is the real-real element of M , and $\Lambda_{qc} = N\Re\bar{h}_{(2)}(0)$.

In the SG phase, we have $q_{EA} > 0$ and $\psi_c = 0$. Therefore, the singular part of Eq. (I.58) yields

$$\tilde{M}_{cc,qq}(0, 0) + \det \mathbf{L}(0) = 0. \quad (\text{I.63})$$

Note that $\det \mathbf{L}(0) = \frac{1}{4Q_{cq}Q_{qc}(0)}$. Corresponding to cases $\frac{1}{2Q_{cq}(0)} = \pm\sqrt{\tilde{M}_{qc,cq}(0, 0)}$, we have

$$\lambda_c^{SG} = -\frac{1}{N} \left(h^d(0) - h^o(0) \right) \pm 2\sqrt{N \times M_{11}(0, 0)}. \quad (\text{I.64})$$

The possibility of $\lambda_c^{SR} = \lambda_c^{SG}$ corresponds to the minus sign of the above equation. Thus we get

$$\lambda_c^{SG} = -\bar{h}_{(1)}(0) + \bar{h}_{(2)}(0) - 2\sqrt{N \times M_{11}(0, 0)}. \quad (\text{I.65})$$

It turns out that the system is in the SR phase rather than the SG phase only if

$$\left(\bar{h}_{(2)}(0) \right)^2 > \frac{1}{N}M_{11}(0, 0). \quad (\text{I.66})$$

This expression also gives the analytical result of the SG-SR phase boundary. In Sec. IF we will elaborate on the calculation for the emitter-graphene system. We find that the values of $\bar{h}_{(2)}(0)$ and $M_{11}(0, 0)$ are insensitive to the graphene Fermi energy E_f .

For the normal phase, λ_c should be determined from the equality

$$\frac{i}{4\pi} \int_{-\infty}^{\infty} d\omega Q_{cc}^{reg}(\omega) = 2. \quad (\text{I.67})$$

The boundaries between the normal phase and the other phases are obtained by matching their values of λ_c .

The determination of q_{EA} and ψ_c , which are present in the singular part of $Q_{cc}(\omega)$, are obtained from the equality

$$\frac{i}{4\pi} \int_{-\infty}^{\infty} d\omega Q_{cc}(\omega) = 2. \quad (\text{I.68})$$

E. Inhomogeneous Broadening

We suppose the emitters suffer from inhomogeneous broadening so that the transition frequency follows a Gaussian distribution

$$\rho(\omega_{i,z}) = \frac{1}{\sqrt{2\pi}\Delta} \exp\left(-\frac{(\omega_{i,z} - \omega_z)^2}{2\Delta^2}\right), \quad (\text{I.69})$$

where Δ is the standard deviation of $\omega_{i,z}$. The corresponding probability distribution of $\frac{1}{\omega_{i,z}}$, is

$$\begin{aligned} p\left(\frac{1}{\omega_{i,z}}\right) &= \omega_{i,z}^2 \rho(\omega_{i,z}) \\ &= \frac{1}{\sqrt{2\pi}\Delta} \exp\left(2\ln\omega_{i,z} - \frac{(\omega_{i,z} - \omega_z)^2}{2\Delta^2}\right). \end{aligned} \quad (\text{I.70})$$

The condition $\Delta \ll \omega_z$ implies that $\ln\omega_{i,z} \approx \ln\omega_z + \omega_{i,z}/\omega_z - 1$. Thus, $1/\omega_{i,z}$ has a Gaussian distribution with variance $\frac{\Delta}{\omega_z^2}$,

$$p\left(\frac{1}{\omega_{i,z}}\right) \approx \frac{\omega_z^2}{\sqrt{2\pi}\Delta} \exp\left(-\frac{(1/\omega_{i,z} - 1/\omega_z)^2}{2(\Delta/\omega_z^2)^2}\right). \quad (\text{I.71})$$

We shall average functions of $\omega_{i,z}$ according to this distribution. Let us rewrite the Keldysh action of the free emitters, Eq. (4) of the main text, but replace ω_z with $\omega_{i,z}$:

$$S_e = - \sum_{i=1}^N \sum_{a=\pm} a \int dt \frac{1}{\omega_{i,z}} (\partial_t \phi_{i,a})^2 + \lambda_{i,a}(t) (\phi_{i,a}^2 - 1). \quad (\text{I.72})$$

Compared with the Keldysh action without inhomogeneous broadening, an additional term is obtained from the average of $\omega_{i,z}$, that is,

$$S^{(b)} = i \frac{\Delta^2}{2\omega_z^4} \sum_{i=1}^N \int_{\omega, \omega'} \omega^2 \omega'^2 \times \phi_{i,c}(-\omega) \phi_{i,q}(\omega) \phi_{i,c}(-\omega') \phi_{i,q}(\omega'). \quad (\text{I.73})$$

Note that the integrals over ω and ω' are independent and factor into a product. We recall that in Eq. (I.41) we made an approximation and released the restriction that $i \neq j$. We can reintroduce the restriction by incorporating the individual terms with $i = j$, and obtain the action

$$S^{(b)} - i \frac{1}{N} \sum_{i=1}^N \int_{\omega, \omega'} v_{ii}^{(a)}(\omega) M_{ab}^o(\omega, \omega') v_{ii}^{(b)}(\omega'). \quad (\text{I.74})$$

To cope with the 4-order terms, we shall apply the Hubbard-Stratonovich transformation.

Let us define $\Phi_{\alpha\beta}^i(\omega, \omega') = \phi_{i,\alpha}(\omega) \phi_{i,\beta}(\omega')$. Then Eq. (I.74) can be rewritten as

$$i \sum_{i=1}^N \int_{\omega, \omega'} \Phi_{\alpha\beta}^i(-\omega, -\omega') \delta \tilde{M}_{\alpha\beta, \alpha'\beta'}(\omega, \omega') \Phi_{\alpha'\beta'}^i(\omega, \omega'). \quad (\text{I.75})$$

where the matrix $\delta \tilde{M}_{\alpha\beta, \alpha'\beta'}(\omega, \omega')$ is defined as

$$\begin{aligned} \delta \tilde{M}_{\alpha\beta, \alpha'\beta'}(\omega, \omega') &= -\frac{1}{N} \tilde{M}_{\alpha\beta, \alpha'\beta'}(\omega, \omega') \\ &+ \omega^2 \omega'^2 \frac{\Delta^2}{8\omega_z^4} (\delta_{\alpha\beta, cq} \delta_{\alpha'\beta', qc} + \delta_{\alpha\beta, qc} \delta_{\alpha'\beta', cq} \\ &+ \delta_{\alpha\beta, cc} \delta_{\alpha'\beta', qq} + \delta_{\alpha\beta, qq} \delta_{\alpha'\beta', cc}). \end{aligned} \quad (\text{I.76})$$

We can implement the Hubbard-Stratonovich transformation of Eq. (I.75) in a way similar to Eq. (I.46):

$$\begin{aligned} &\int D[Q_a^i] e^{-N \int_q Q_a^i(-q) \tilde{M}_{ab}(q) Q_b^i(q) - 2i \int_q Q_a^i(-q) \tilde{M}_{ab}(q) \Phi_b(q)} \\ &\propto e^{-\frac{1}{N} \int_q \Phi_a^i(-q) \tilde{M}_{ab}(q) \Phi_b^i(q)}, \end{aligned} \quad (\text{I.77})$$

where the conventions of notation are the same as in Eq. (I.46). In the sense of saddle-point equations, the physical meaning of $Q_{\alpha\beta}^i$ is

$$Q_{\alpha\beta}^i = \langle \phi_{i,\alpha} \phi_{i,\beta} \rangle \quad (\text{I.78})$$

By the further assumption of the homogeneous mean-field ansatz, that for $\forall i$,

$$\langle \phi_{i,\alpha} \phi_{i,\beta} \rangle = \frac{1}{N} \sum_{k=1}^N \langle \phi_{k,\alpha} \phi_{k,\beta} \rangle, \quad (\text{I.79})$$

we can replace the new variable $Q_{\alpha\beta}^i$ with $Q_{\alpha\beta}$, which is defined in the context of spatial disorders.

The result of all the above steps can also be obtained by rewriting Eq. (I.74) as

$$i \frac{1}{N} \int_{\omega, \omega'} \Phi_{\alpha\beta}(-\omega, -\omega') \delta \tilde{M}_{\alpha\beta, \alpha'\beta'}(\omega, \omega') \Phi_{\alpha'\beta'}(\omega, \omega') \quad (\text{I.80})$$

followed by the Hubbard-Stratonovich transformation in a way similar to Eq. (I.46). It means that, the effect of inhomogeneous broadening can be seen as a modification of the matrix \tilde{M} defined in Eq. (I.43) by a term $\delta \tilde{M}$ given in Eq. (I.75).

Note that the first term of Eq. (I.75) comes from the additional term mentioned in Eq. (I.74) and contributes only little when $N \gg 1$, thus justifying the approximation made for Eq. (I.43). Since \tilde{M} is defined with a factor of N , see Eq. (I.40), the correction made by inhomogeneous broadening, Eq. (I.76), is also negligible when N is large.

F. The specific example of the Emitter-Graphene System

The surface conductivity of the graphene monolayer is

$$\begin{aligned} \sigma(E_f, \tau; \omega) &= \frac{e^2 E_f}{\pi \hbar^2} \frac{i}{\omega + i\tau^{-1}} \\ &+ \frac{e^2}{4\hbar} \left(\Theta(\hbar\omega - 2E_f) + \frac{i}{\pi} \log \left| \frac{\hbar\omega - 2E_f}{\hbar\omega + 2E_f} \right| \right). \end{aligned} \quad (\text{I.81})$$

When the emitter dipoles are aligned perpendicular to the graphene monolayer, the relevant element of the dyadic Green's tensor is $\mathbf{G}_{zz}^0 + \mathbf{G}_{zz}^s$, where \mathbf{G}_{zz}^0 is the vacuum dyadic Green's function for free propagation modes and \mathbf{G}_{zz}^s is the so-called 'scattering' part accounting for the surface plasmon modes of the graphene monolayer

$$\begin{aligned} \frac{\omega^2}{c^2} \mathbf{G}_{zz}^s(r, r'; z) &= \int \frac{d^2 \mathbf{k}_\parallel}{(2\pi)^2} \frac{i}{2\epsilon_1 k_{1,z}} k_\parallel^2 r_p e^{i\mathbf{k}_\parallel \cdot \delta \mathbf{r} + 2ik_{1,z} z} \\ &= \int \frac{dk_\parallel}{2\pi} \frac{i}{2\epsilon_1 k_{1,z}} k_\parallel^3 r_p J_0(k_\parallel \delta r), e^{2ik_{1,z} z} \end{aligned} \quad (\text{I.82})$$

where $\delta \mathbf{r} = \mathbf{r} - \mathbf{r}'$ and δr is its length; J_0 is the zero-order Bessel function; $\epsilon_{1(2)}$ is the relative permittivity of the dielectric above(below) the graphene monolayer, r_p is the Fresnel coefficient of reflection of the p-modes from above the graphene layer

$$r_p = \frac{-\epsilon_1 k_{2,z} + \epsilon_2 k_{1,z} + \frac{\sigma(\omega)}{\omega \epsilon_0} k_{1,z} k_{2,z}}{\epsilon_1 k_{2,z} + \epsilon_2 k_{1,z} + \frac{\sigma(\omega)}{\omega \epsilon_0} k_{1,z} k_{2,z}}, \quad (\text{I.83})$$

where $k_{1(2),z} = \sqrt{\frac{\omega^2}{c^2} \epsilon_{1(2)} - k_\parallel^2}$. Note that in the limit $\omega \rightarrow 0$, r_p equals 1 and does not depend on the Fermi energy. As a result, the Fermi energy E_f is irrelevant to the SG-SR boundary.

In the numerical calculation, it is convenient to normalize k_\parallel and δr in the above expressions by ω_z/c . That

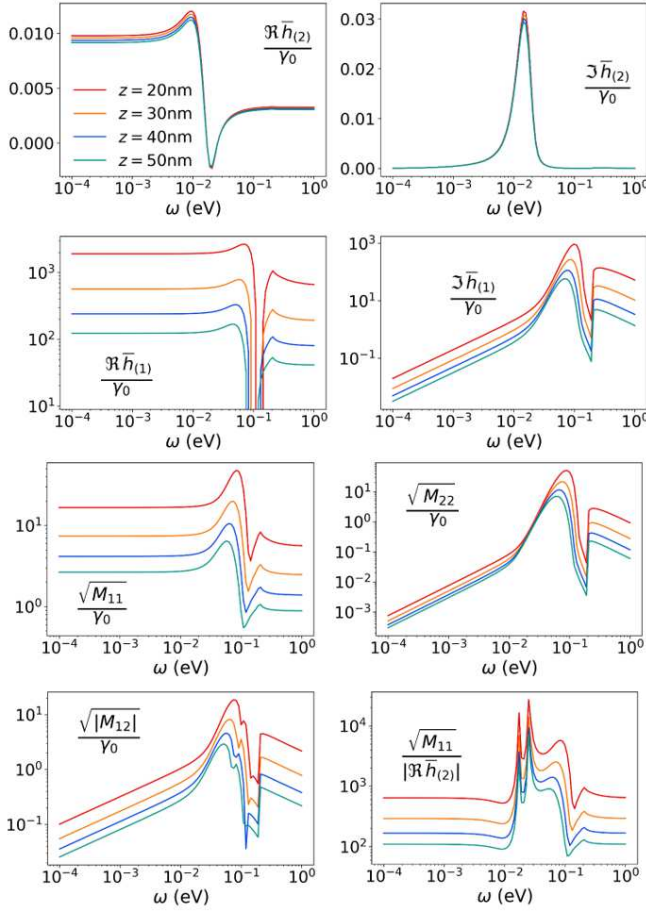


Figure I.4. Coefficients of the emitter-graphene surface plasmon coupling, for systems with $\omega_z = 0.5$ eV, $E_f = 0.1$ eV, and $L = 10^3$ nm. From top to the bottom in the figures we show results for the different heights $z=20$ (red), 30 (orange), 40 (blue) and 50 (green) nm. The dimensionless values are normalized by the emitter spontaneous emission rate γ_0 .

is, define

$$k_{||} = \frac{\omega}{c} \tilde{k}_{||}, \quad \delta r = \frac{c}{\omega_z} \delta \tilde{r}, \quad z = \frac{c}{\omega_z} \tilde{z}, \quad (\text{I.84})$$

and then Eq. (I.82) is recast to

$$\left(\frac{\omega_z}{c}\right)^3 \int_0^\infty \frac{d\tilde{k}_{||}}{2\pi} \frac{i}{2\epsilon_1 \tilde{k}_{1,z}} \tilde{k}_{||}^3 r_p J_0(\tilde{k}_{||} \delta \tilde{r}) e^{2i\tilde{k}_{1,z} \tilde{z}}. \quad (\text{I.85})$$

The factor $(\frac{\omega_z}{c})^3$ can then be combined with the length of \mathbf{d}_i and absorbed into the expression for the vacuum spontaneous emission rate γ_0 .

The surface-plasmons have the dispersion relation

$$\epsilon_1 k_{2,z}^{sp} + \epsilon_2 k_{1,z}^{sp} + \frac{\sigma(\omega_{sp})}{\omega_{sp} \epsilon_0} k_{1,z}^{sp} k_{2,z}^{sp} = 0, \quad (\text{I.86})$$

where $k_{1(2),z} = \sqrt{\frac{\omega^2}{c^2} \epsilon_{1(2)} - k_{sp}^2}$, ω_{sp} and k_{sp} represent the frequency and wavevector of the surface-plasmon, respectively.

The horizontal coordinates $\{(x_i, y_i)\}_i$ of the emitters are assumed to follow the identical Gaussian distribution

$$p(x, y) = \frac{1}{2\pi L^2} \exp\left(-\frac{x^2 + y^2}{2L^2}\right), \quad (\text{I.87})$$

and the distance between any two emitters follows the distribution

$$p_L(\delta r) = \frac{\delta r}{2L^2} \exp\left(-\frac{(\delta r)^2}{4L^2}\right). \quad (\text{I.88})$$

To calculate the mean values and covariances $\bar{h}_{(1)}(\omega)$, $\bar{h}_{(2)}(\omega)$ and $\bar{M}(\omega, \omega')$ required in our formalism, the use of the Gaussian distribution permits analytical handling of the oscillating integrands related to the Bessel function $J_0(k\delta r)$.

$$\begin{aligned} \int_0^\infty dr \frac{r}{2L^2} J_0(kr) \exp\left(\frac{-r^2}{4L^2}\right) &= \exp(-k^2 L^2), \\ \int_0^\infty dr \frac{r}{2L^2} J_0(kr) J_0(k'r) \exp\left(-\frac{r^2}{4L^2}\right) &= \\ I_0(2L^2 k k') \exp\left(-L^2(k^2 + k'^2)\right). \end{aligned} \quad (\text{I.89})$$

where I_0 is the modified Bessel function. By use of these formulas, the remaining integrals are numerically well behaved.

Finally, to have an impression of the numerical results, we illustrate the z -dependence of the averaged coupling strength and the elements of the covariance matrix in Fig. 4. It shows that by decreasing z , the graphene SP-induced self-interaction terms and the elements of the covariance matrix are increased significantly, while the SP-induced emitter-emitter coupling strength changes little. It confirms our argument about the z -dependence made in the main text.